

# ZFP36 ring finger protein like 1 significantly suppresses human coronavirus OC43 replication

Tooba Momin<sup>1</sup>, Andrew Villasenor<sup>1</sup>, Amit Singh<sup>1</sup>, Mahmoud Darweesh<sup>2</sup>, Aditi Singh<sup>1</sup>, Mrigendra Rajput<sup>Corresp. 1</sup>

<sup>1</sup> Department of Biology, University of Dayton, Dayton, Ohio, United States

<sup>2</sup> Department of Medical Biochemistry and Microbiology, Uppsala University, Uppsala, Uppsala, Sweden

Corresponding Author: Mrigendra Rajput  
Email address: mrajput1@udayton.edu

CCCH-type Zinc finger proteins (ZFP) are small cellular proteins that are structurally maintained by zinc ions. Zinc ions coordinate the protein structure in a tetrahedral geometry by binding to cysteine- cysteine or cysteines - histidine amino acids. ZFP's unique structure enables it to interact with a wide variety of molecules including RNA; thus, ZFP modulates several cellular processes including the host immune response and virus replication. CCCH-type ZFPs have shown their antiviral efficacy against several DNA and RNA viruses. However, their role in the human coronavirus is little explored. We hypothesized that ZFP36L1 also suppresses the human coronavirus. To test our hypothesis, we used OC43 human coronavirus (HCoV) strain in our study. We overexpressed and knockdown ZFP36L1 in HCT-8 cells using lentivirus transduction. Wild type, ZFP36L1 overexpressed, and ZFP36L1 knockdown cells were each infected with HCoV-OC43, and the virus titer in each cell line was measured over 96 hours post-infection (p.i.). Our results show that HCoV-OC43 replication was significantly reduced with ZFP36L1 overexpression while ZFP36L1 knockdown significantly enhanced virus replication. ZFP36L1 knockdown HCT-8 cells started producing infectious virus at 48 hours p.i. which was an earlier timepoint as compared to wild -type and ZFP36L1 overexpressed cells. Wild-type and ZFP36L1 overexpressed HCT-8 cells started producing infectious virus at 72 hours p.i.. Overall, the current study showed that overexpression of ZFP36L1 suppressed human coronavirus (OC43) production.

1 ZFP36 Ring Finger Protein Like 1 significantly suppresses  
2 Human coronavirus OC43 replication

3

4 Tooba Momin<sup>1</sup>, Andrew Villasenor<sup>1</sup>, Amit Singh<sup>1</sup>, Mahmoud Darweesh<sup>2</sup>, Aditi Singh<sup>1</sup>,  
5 Mrigendra Rajput<sup>1</sup>

6

7

8 <sup>1</sup>Department of Biology, University of Dayton, Dayton, Ohio, USA 45469

9 <sup>2</sup>Department of Medical Biochemistry and Microbiology, Uppsala University, Uppsala, Sweden,

10 75105

11

12

13 Corresponding Author:

14 Mrigendra Rajput

15 SC 234, Department of Biology, 300 College Street, University of Dayton, Dayton, Ohio, 45469,

16 USA

17

18

19

20

21

22

23

24

25

26

27

28

29

30

31

32

33

34

35

36

37

**38 Abstract**

39 CCCH-type Zinc finger proteins (ZFP) are small cellular proteins that are structurally maintained  
40 by zinc ions. Zinc ions coordinate the protein structure in a tetrahedral geometry by binding to  
41 cystine- cystine or cysteines - histidine amino acids. ZFP's unique structure enables it to interact  
42 with a wide variety of molecules including RNA; thus, ZFP modulates several cellular processes  
43 including the host immune response and virus replication. CCCH-type ZFPs have shown their  
44 antiviral efficacy against several DNA and RNA viruses. However, their role in the human  
45 coronavirus is little explored. We hypothesized that ZFP36L1 also suppresses the human  
46 coronavirus. To test our hypothesis, we used OC43 human coronavirus (HCoV) strain in our  
47 study. We overexpressed and knockdown ZFP36L1 in HCT-8 cells using lentivirus transduction.  
48 Wild type, ZFP36L1 overexpressed, and ZFP36L1 knockdown cells were each infected with  
49 HCoV-OC43, and the virus titer in each cell line was measured over 96 hours post-infection  
50 (p.i.).

51 Our results show that HCoV-OC43 replication was significantly reduced with ZFP36L1  
52 overexpression while ZFP36L1 knockdown significantly enhanced virus replication. ZFP36L1  
53 knockdown HCT-8 cells started producing infectious virus at 48 hours p.i. which was an earlier  
54 timepoint as compared to wild -type and ZFP36L1 overexpressed cells. Wild-type and ZFP36L1  
55 overexpressed HCT-8 cells started producing infectious virus at 72 hours p.i.. Overall, the  
56 current study showed that overexpression of ZFP36L1 suppressed human coronavirus (OC43)  
57 production.

58

59

60

61

62 Keywords: CCCH type Zinc finger protein, ZFP36L1, RNA binding protein, human coronavirus  
63 OC43

**64 Introduction**

65 ZFPs are small cellular proteins that are structurally maintained by zinc ions. Zinc ions coordinate  
66 the protein structure in a tetrahedral geometry (Abbehausen, 2019; Hajikhezri, 2020). There are  
67 over 40 different types of ZFPs that have been annotated so far (Hajikhezri, 2020). ZFP's unique  
68 structure enables it to interact with a wide variety of molecules such as DNA, RNA, PAR (poly-  
69 ADP-ribose), and cellular proteins and thus modulate several cellular processes including host  
70 immune response and virus replication (Müller et al., 2007; Cassandri et al., 2017; Takata et al.,  
71 2017; Tang, Wang & Gao, 2017; Meagher et al., 2019; Lal, Ullah & Syed, 2020). Among various  
72 ZFPs, the CCCH-type ZFP family contains zinc ions that coordinate protein structure by binding  
73 to cystine-cystine or cysteines-histidine amino acids (Abbehausen, 2019; Hajikhezri, 2020). The  
74 CCCH-type ZFP family has also been characterized for its antiviral (Hajikhezri, 2020; Tang, Wang  
75 & Gao, 2017; Zhang, et al., 2020; Guo et al., 2004; Zhao et al., 2019; Gao, Guo & Goff, 2002;  
76 Zhu et al., 2020; Musah, 2004; Chen, Jeng & Lai, 2017; Scozzafava et al., 2003; Schito et al.,  
77 2006; Angiolilli et al., 2021) and immune modulator activity (Wang et al., 2015; Tu et al., 2019;  
78 Haneklaus et al., 2017; Lv et al., 2021; Matsushita et al., 2009; Wawro, Kochan & Kasza, 2016;  
79 Uehata, & Akira, 2013; Chen et al., 2018; Mino et al., 2015; Fu & Blackshear, 2017; Stumpo,  
80 Lai & Blackshear, 2010; Shrestha, Pun & Park, 2018; Kontoyiannis, 2018).

81 CCCH-type ZFPs show their antiviral efficacy against several RNA viruses including Influenza A  
82 virus (Tang, Wang & Gao, 2017), retrovirus (Gao, Guo & Goff, 2002; Zhu et al., 2011; Zhu et al.,  
83 2017) filoviruses (Müller, 2007), and alphavirus such as Sindbis virus, Semliki Forest virus, Ross  
84 River virus, and Venezuelan equine encephalitis virus (Bick et al., 2003). However, CCCH-type  
85 ZFP's role on the human coronavirus is little explored. The current study is designed to evaluate  
86 the effect of ZFP36L1, a CCCH-type ZFP, on human coronavirus (HCoV)-OC43 replication.

**87 Materials & Methods**

88

**89 Cells, Virus Strains and Virus Propagation**

90 HCT-8 cells (ATCC, Manassas, VA) were cultured in Roswell Park Memorial Institute (RPMI)  
91 1640 Medium (Gibco BRL, Grand Island, NY) and supplemented with 10% heat-inactivated  
92 fetal bovine serum (FBS), (ATCC, Manassas, VA), and antibiotic-antimycotic: penicillin 100  
93 units /ml, streptomycin 0.10 mg /ml and amphotericin B 0.25 µg /ml (Sigma-Aldrich, St. Louis,  
94 MO). During virus culture, HCT-8 cells were adapted to 1% FBS. HCT-8 cells cultured with  
95 RPMI 1640 medium supplemented with 1% FBS were used to grow and subsequently titrate the  
96 OC43 human coronavirus (HCoV) stain (ATCC, Manassas, VA).

**97 Overexpression and knockdown of ZFP36L1**

98 HCT-8 cells were stably overexpressed for ZFP36L1 (NCBI reference sequence:  
99 NM\_001244701.1) with a green fluorescent protein (GFP) marker using a lentivirus vector. The  
100 ZFP36L1 gene containing both tandem zinc finger domains (TZFD) such as TZFD1 and TZFD2  
101 were cloned in a pLV-eGFP plasmid with the help of Vector Builder Inc, IL. To make the  
102 lentivirus, pLV-eGFP plasmids containing our gene of interest were co-transfected with VSV-G  
103 and packaging plasmids encoding Gag/Pol and Rev in HEK293T cells. After 48 hours, the  
104 supernatant containing the lentivirus was collected and purified by centrifugation followed by  
105 filtration. Purified lentivirus was concentrated using a sucrose gradient ultracentrifugation and  
106 this concentrated, purified lentivirus was used in the study.

107 Similar to ZFP36L1 overexpression, HCT-8 cells were knockdown for ZFP36L1 using ZFP36L1  
108 specific shRNA (GTAACAAGATGCTCAACTATA). The ZFP36L1 shRNA was stably  
109 expressed using a lentivirus by cloning it in a pLV-mCherry plasmid. Lentivirus for ZFP36L1-

110 shRNA was prepared as per the above-mentioned method by co-transfection of pLV-mCherry  
111 containing ZFP36L1 shRNA with VSV-G and packaging plasmids in HEK293T cells.  
112 The prepared lentiviruses were used to either overexpress or knock down ZFP36L1. Successful  
113 lentivirus transduction was measured through GFP or mCherry expression for ZFP36L1  
114 overexpression (GFP) or ZFP36L1 knockdown (mCherry), respectively. Transduced HCT-8 cells  
115 were selected with an increased concentration of puromycin (2-3  $\mu\text{g}/\text{ml}$ ) over 7 days. Selected  
116 cells were further characterized for ZFP36L1 overexpression or knockdown using a western blot  
117 with ZFP36L1-specific antibodies.

#### 118 **Western blot analysis for ZFP36L1 expression**

119 To confirm ZFP36L1 overexpression or ZFP36L1 knockdown; wild type, ZFP36L1  
120 overexpressed and ZFP36L1 knockdown HCT-8 cells were individually seeded in T25 flasks.  
121 When cells reached 75-80% confluency, cells were lysed using a radioimmunoprecipitation  
122 assay buffer (RIPA buffer) (Cell Signaling Technology, Danvers, MA) supplemented with  
123 protease-phosphatase inhibitor (Cell Signaling Technology, Danvers, MA). Lysates were then  
124 centrifuged at 3000 X g for 15 minutes at 4 °C. The supernatant was collected and the protein  
125 concentration in each supernatant was measured using the Pierce™ BCA Protein Assay Kit  
126 (Thermo Fisher Scientific, Waltham, MA). 40  $\mu\text{g}$  cell lysates were separated through 12%  
127 resolving SDS PAGE gel. After separation, proteins were transfected onto a polyvinylidene  
128 difluoride (PVDF) membrane (Thermo Fisher Scientific, Waltham, MA). The PVDF membrane  
129 was blocked with 5% skimmed milk (Sigma-Aldrich, St. Louis, MO) in Tris-buffered saline  
130 (TBS) for 1 hour at room temperature followed by incubation with anti- ZFP36L1 antibody  
131 (1:1000) (Thermo Fisher Scientific, Waltham, MA) and anti-  $\beta$ actin antibody (1:4000) (Cell  
132 Signaling Technology, Danvers, MA) overnight at 4 °C. After overnight incubation, membranes

133 were washed with tris-buffered saline +0.1% Tween 20 (TBST) and incubated with HRP  
134 conjugated secondary antibodies (1:2000) for 1 hour at room temperature. After washing,  
135 membranes were developed using the Pierce ECL Western Blotting Substrate (Thermo Fisher  
136 Scientific, Waltham, MA). Images of the western blot were taken by the Odyssey XF Imaging  
137 System (LI-COR Biosciences, Lincoln, NE). Band intensity for ZFP36L1 proteins was  
138 normalized with  $\beta$ -actin using ImageJ software (Schneider, Rasband & Eliceiri, 2012) A  
139 significant difference in ZFP36L1 expression in ZFP36L1 overexpressed and knockdown cells  
140 compared to wild-type cells was estimated using a paired T-test.

#### 141 **Determining ZFP36L1's effect on HCT-8 cells viability**

142 The effect of ZFP36L1 overexpression and its knockdown on cell viability was measured by  
143 trypan blue exclusion assay (Strober, 2015). Wild type, ZFP36L1 overexpressed and ZFP36L1  
144 knockdown cells were individually seeded in 6 well plates ( $1.5 \times 10^6$  cell/well) in triplicate. 96  
145 hours post-seeding, cells were washed with sterilized phosphate-buffered saline (PBS) and  
146 detached with 0.25% trypsin-EDTA (ATCC, Manassas, VA). Detached cells were washed with  
147 PBS by centrifugation at 500x g for 5 minutes at 4 °C, and then cells were stained with 0.4%  
148 trypan blue for 3 minutes and examined for cell. Changes in cell viability following ZFP36L1  
149 overexpression or its knockdown compared to wild-type cells was estimated by paired t-test.

#### 150 **Measuring the effect of ZFP36L1 expression on virus titration**

151 Wild type, ZFP36L1 overexpressed and ZFP36L1 knockdown HCT-8 cells were infected with  
152 HCoV-OC43 with 0.1 multiple of infection (MOI) individually. The supernatant from these cells  
153 was collected at 24 hours, 48 hours, 72 hours, and 96 hours p.i. Collected cell supernatants were  
154 then centrifuged at 1000Xg at 4°C for 15 minutes to remove cell debris and stored at -80 ° C  
155 until used. Once samples from all time points were collected, the HCoV-OC43 virus titer was

156 determined as per the aforementioned method (Reed & Muench, 1938). Changes in virus titer in  
157 ZFP36L1 overexpressed or ZFP36L1 knockdown cells were compared to wild-type cells and  
158 statistically analyzed by a paired T-test.

### 159 **Measuring the effect of ZFP36L1 expression on HCoV-OC43 replication.**

160 To measure the effect of ZFP36L1 overexpression or ZFP36L1 knockdown on HCoV-OC43  
161 replication, we infected ZFP36L1 overexpressed, ZFP36L1 knockdown or wild type HCT-8 cells  
162 with HCoV-OC43 (MOI: 0.1). Infected cells were collected at 72 and 96 hours p.i. Viral RNA  
163 was isolated from infected cells using the QIAamp Viral RNA Mini kit (Qiagen, Valencia, CA,  
164 USA). The viral nucleocapsid was quantified using qPCR (Stratagene MX3000P Real-Time  
165 Thermocycler, Stratagene Inc., La Jolla, USA) in 25 µl reaction using syber green dye. Primer  
166 sequence for nucleocapsid (F: 5'-: GCTGTT TWTGTTAAG TCYAAA GT-3', R: 5'-  
167 ATTCTGATAGAGAGTGCYTAT Y-3') were used (Al-Khannaq, et al., 2016) with qPCR  
168 amplification cycle at 95°C/ 2 minutes, 40 cycles of (95 °C/15 and 60 °C/ 1 minutes) followed  
169 by melting curve cycle at: 95°C/ 15 seconds, 60°C/ 1 minute and 95°C/ 15 seconds. Fold change  
170 in HCoV nucleocapsid expression in each cell was estimated by paired -test.

### 171 **Statistical analysis**

172 The significant change in HCoV-OC43 titer and virus replication in wild-type, ZFP36L1  
173 overexpressed, or ZFP36L1 knockdown cells was estimated using a paired T-test with 95%  
174 degree of freedom. Virus titer in wild-type, ZFP36L1 overexpression or ZFP36L1 knockdown  
175 cells was repeated at least three times with calculations for average, standard deviation, and  
176 standard error.

177

### 178 **Results**

179

180 **ZFP36L1 was overexpressed or knockdown in HCT-8 cells.**

181 A stable ZFP36L1 overexpression with an upstream GFP marker in HCT-8 cells was generated  
182 using a lentivirus system. GFP expression in HCT-8 cells was considered positive for ZFP36L1  
183 overexpression (Figure 1B), which was further confirmed by western blot (Figure 2 and Figure  
184 3). Similarly, ZFP36L1 was knockdown using ZFP36L1-specific shRNA. The shRNA was  
185 located downstream to mCherry and expression of ZFP36L1-specific shRNA was determined by  
186 mCherry expression (Figure 1C) and ZFP36L1 knockdown was confirmed by western blot  
187 analysis (Figure 2 and Figure 3). Our results showed that lentivirus significantly overexpressed  
188 or knockdown ZFP36L1 in HCT-8 cells ( $p < 0.05$ ) (Figure 2 and Figure 3).

189

#### 190 **ZFP36L1 overexpressing or its knockdown did not affect HCT-8 cells' viability**

191 The effect of ZFP36L1 overexpression or its knockdown was measured on HCT-8 cells' viability  
192 using trypan blue exclusion assay. Results showed that overexpression or knockdown of  
193 ZFP36L1 in HCT-8 cells did not affect its viability. Wild type, ZFP36L1 overexpressed and  
194 ZFP36L1 knockdown cells showed viability as  $94.83 \pm 1.01\%$ ,  $94.16 \pm 0.71\%$ , and  $95.83 \pm 0.43\%$  at  
195 96 hours post seeding, respectively. These values were non-significant different to each other  
196 ( $p < 0.05$ ) (Figure 4). Additionally, no apparent morphological changes were observed among  
197 these cells.

#### 198 **ZFP36L1 overexpression significantly suppressed, while ZFP36L1 knockdown** 199 **significantly enhanced the HCoV-OC43 production.**

200 Wild type, ZFP36L1 overexpressed, and ZFP36L1 knockdown HCT-8 cells were infected  
201 individually with HCoV-OC43 with a MOI of 0.1. Cell supernatants were collected at 24 hours,  
202 48 hours, 72 hours, and 96 hours p.i. and analyzed for virus titer.

203 Results showed that ZFP36L1 overexpression in HCT-8 cells significantly reduced virus titer  
204 ( $p < 0.05$ ) (Figure 5). Virus titer in ZFP36L1 overexpressed cells ion was  $2.24 \pm 1.28 \log_{10}/\text{ml}$  and  
205  $4.32 \pm 0.00 \log_{10}/\text{ml}$  at 72 hours and 96 hours p.i. respectively. These titer values were  
206 significantly lower than virus titers in wild-type cells at same time points, such as 72 hours p.i.  
207 ( $4.08 \pm 0.11 \log_{10}/\text{ml}$ ) and 96 hours p.i. ( $5.42 \pm 0.10 \log_{10}/\text{ml}$ ) ( $p < 0.05$ ) (Figure 5).

208 Results with ZFP36L1 knockdown HCT-8 cells showed that ZFP36L1 knockdown significantly  
209 enhanced virus titer ( $p < 0.05$ ) (Figure 5). Knocking down ZFP36L1 facilitated the infectious  
210 virus production as early as 48 hours p.i. while wild-type cells produced infectious viruses at 72  
211 hours p.i. The virus titer in ZFP36L1 knockdown cells was recorded as  $00.00 \pm 0.00 \log_{10}/\text{ml}$ ,  
212  $2.86 \pm 0.00 \log_{10}/\text{ml}$ ,  $4.52 \pm 0.22 \log_{10}/\text{ml}$ , and  $5.85 \pm 0.01 \log_{10}/\text{ml}$  at 24 hours, 48 hours, 72  
213 hours and 96 hours p.i., respectively. While wild-type HCT-8 cells have virus titer of  $0.00 \pm 0.00$   
214  $\log_{10}/\text{ml}$ ,  $0.00 \pm 0.00 \log_{10}/\text{ml}$ ,  $4.08 \pm 0.11 \log_{10}/\text{ml}$ , and  $5.42 \pm 0.10 \log_{10}/\text{ml}$  at 24 hours, 48  
215 hours, 72 hours and 96 hours p.i., respectively. Virus titer in ZFP36L1 knockdown cells was  
216 significantly higher at 48 hours and 96 hours p.i compared to wild-type cells ( $p < 0.05$ ) (Figure 5).  
217 Results also showed a lower cytopathic effect in ZFP36L1 overexpressed or wild-type HCT-8  
218 cells compared to ZFP36L1 knockdown cells at 72 hours p.i. (Figure 6)

219 **ZFP36L1 overexpression significantly suppressed while ZFP36L1 knockdown significantly**  
220 **enhanced the HCoV-OC43 RNA replication.**

221 To further confirm ZFP36L1's effect on HCoV-OC43 RNA replication, wild type, ZFP36L1  
222 overexpressed and ZFP36L1 knockdown HCT-8 cells were individually infected with HCoV-  
223 OC43 (MOI: 0.1). Infected cells were collected at 72 and 96 hours p.i. Viral RNA was isolated  
224 from infected cells and viral nucleocapsid transcription (RNA concentration) was analyzed using  
225 qPCR. Results showed a significant increase in HCoV-OC43 nucleocapsid expression at 72

226 hours and 96 hours p.i. in ZFP36L1 knockdown HCT-8 cells while ZFP36L1 overexpression  
227 significantly suppressed HCoV-OC43 nucleocapsid expression at both of these time points  
228 (e.g. 72 and 96 hours p.i.) ( $p < 0.05$ ). ZFP36L1 knockdown HCT-8 cells displayed a  $3.56 \pm 0.77$  and  
229  $7.67 \pm 1.69$ -fold increase in HCoV-OC43 nucleocapsid expression as compared to wild-type  
230 HCT-8 cells at 72 hours and 96 hours p.i., respectively (Figure 7). While ZFP36L1  
231 overexpressed cells displayed a significantly lower HCoV-OC43 nucleocapsid expression such  
232 as  $0.38 \pm 0.16$  and  $0.16 \pm 0.03$  fold compared to wild-type cells at 96 hours p.i. ( $p < 0.05$ ) (Figure 7).

### 233 **Discussion**

234 The current study was designed to determine the role of ZFP36L1 (a CCCH type ZFP) on  
235 HCoV-OC43 replication. Our results showed that overexpression of ZFP36L1 significantly  
236 reduced infectious HCoV-OC43 production while ZFP36L1 knockdown significantly enhanced  
237 virus titer compared to wild-type cells. ZFP36L1 overexpression also reduced the RNA  
238 replication of HCoV-OC43 and suppressed the apparent cytopathic effect in infected cells.  
239 ZFPs are one of the most abundant proteins in humans which can make up to 5% of total human  
240 proteins (Vilas et al., 2018). ZFPs have an extremely high binding ability. They can bind to cellular  
241 DNA, RNA, lipids, proteins, and PAR (poly-ADP-ribose); therefore, ZFPs can modulate several  
242 cellular types of machinery (Müller et al., 2007; Cassandri et al., 2017; Takata et al., 2017; Tang,  
243 Wang & Gao, 2017; Vilas et al., 2018; Meagher et al., 2019; Lal, Ullah & Syed, 2020). The diverse  
244 binding properties of ZFPs make it difficult to characterize their functional effect in cells (Vilas et  
245 al., 2018). However, such a challenge is overcome by classifying the ZFPs and then identifying  
246 their functional characteristics (Cassandri et al., 2017). Classification of ZFP is based on zinc ion,  
247 zinc ion interaction with specific amino acids, and the protein's folded structure (Krishna,  
248 Majumdar & Grishin, 2003). Based on such classification, CCCH-type ZFP is characterized to

249 interact with RNA and thus modulate RNA metabolism in the cell (Maeda & Akira, 2017).  
250 including interfering with RNA virus replication (Gao, Guo & Goff, 2002; Cassandri et al., 2017).  
251 The known mechanisms by which CCCH-type ZFPs exhibit these antiviral or immunomodulatory  
252 activities is by limiting the total mRNA turnover in the cell. CCCH-type ZFPs such as ZFP36L1  
253 have two tandem zinc finger (TZF) domains that are known to bind with adenyl and uracyl  
254 nucleotides-rich (AU-rich) elements (AREs) in mRNA. This interaction facilitates RNA  
255 degradation by CCR4-NOT complex-mediated deadenylation, followed by 5' decapping and  
256 exonuclease-mediated nucleotide cleaving (Blackshear, 2002; Lai, Kennington & Blackshear,  
257 2003; Lykke-Andersen & Wagner, 2005; Suk et al., 2018; Lai et al., 2019; Lai et al., 2000).  
258 Coronavirus genome, including HCoV-OC43's genome is 5'-capped with a 3' poly(A) tail of  
259 variable length (Fehr & Perlman, 2015). The length of the poly (A) tail varies at different stages  
260 of the virus replication cycle and viruses with longer poly (A) tails replicate at a faster rate (Wu et  
261 al., 2013). Therefore, the effect of ZFP36L1 on viral poly (A) may explain reduced virus  
262 production with ZFP36L1 overexpression in the current study. Our study not only showed that  
263 ZFP36L1 suppressed the infectious HCoV-OC43 production, but also reduced HCoV-OC43  
264 nucleocapsid transcription indicating that ZFP36L1 mediates its antiviral effect by limiting the  
265 viral RNA in infected cells.

266 However, there is the possibility that ZFP36L1 can reduce virus replication with different  
267 mechanisms other than poly A tail interaction. A study showed that CCCH Type ZFP also targets  
268 the non-ARE sequence of 3' and 5' (untranslated region) UTR in mRNA (Li et al., 2015). While  
269 another study showed that CCCH Type ZFP targets CG-rich viral sequences (Meagher et al.,  
270 2019). The study also showed that ZFP36 (ZFP36L1) suppressed the virus production (influenza  
271 A virus) by interfering with viral protein translation/ export from the nucleus to the cytoplasm

272 without affecting viral RNA replication (Lin et al., 2020). Therefore, a detailed study to determine  
273 ZFP36L1's mechanism of action for suppressing coronavirus replication needs to be explored.

274

## 275 **Conclusions**

276 The current study showed that overexpression of ZFP36L1, a CCCH type ZFP significantly  
277 reduced HCoV-OC43 RNA (nucleocapsid) and infectious virus production. A reduced viral  
278 production was in correlation with reduced cytopathic effect in the infected cells. Furthermore,  
279 ZFP36L1 knockdown significantly enhanced the HCoV-OC43 replication and infectious virus  
280 production. However, additional mechanisms employed to reduce virus replication still need to  
281 be explored.

282

## 283 **Acknowledgments**

284 The author thanks the Department of Biology, University of Dayton, Ohio, USA, for providing  
285 support to conduct the current research.

286

## 287 **References**

288

- 289 1. Abbehausen C. 2019. Zinc finger domains as therapeutic targets for metal-based  
290 compounds - an update. *Metallomics* 11(1): 15-28.
- 291 2. Al-Khannaq MN, Ng KT, Oong XY, Pang YK, Takebe Y, Chook JB, Hanafi NS,  
292 Kamarulzaman A, Tee KK. 2016. Molecular epidemiology and evolutionary histories  
293 of human coronavirus OC43 and HKU1 among patients with upper respiratory tract  
294 infections in Kuala Lumpur, Malaysia. *Virology Journal*. 25;13:33. doi:  
295 10.1186/s12985-016-0488-4. PMID: 26916286; PMCID: PMC4766700.
- 296 3. Angiolilli C, Leijten EFA, Bekker CPJ, Eeftink E, Giovannone B, Nordkamp MO, van  
297 der Wal M, Thijs JL, Vastert SJ, van Wijk F, Radstake TRDJ and van Loosdregt J.  
298 2021. ZFP36 family members regulate the pro-inflammatory features of psoriatic  
299 dermal fibroblasts. *Journal of Investigative Dermatology*. 142(2):402-413
- 300 4. Bick MJ, Carroll JW, Gao G, Goff SP, Rice CM, MacDonald MR. 2003. Expression  
301 of the zinc-finger antiviral protein inhibits alphavirus replication. *Journal of*  
302 *Virology*.77(21):11555-62. doi: 10.1128/jvi.77.21.11555-11562.2003. PMID:  
303 14557641; PMCID: PMC229374.
- 304 5. Blackshear, PJ. 2002. Tristetraprolin and other CCCH tandem zinc-finger proteins in  
305 the regulation of mRNA turnover. *Biochemical Society Transactions*. 30(6): 945-52.

- 306 6. Cassandri M, Smirnov A, Novelli F, Pitolli C, Agostini M, Malewicz M, Melino G,  
307 Raschellà G. 2017. Zinc-finger proteins in health and disease. *Cell Death Discovery*.  
308 13;3:17071. doi: 10.1038/cddiscovery.2017.71. PMID: 29152378; PMCID:  
309 PMC5683310.
- 310 7. Cassandri MA, Smirnov F, Novelli C, Pitoll M, Agostini M, Malewicz GG., Raschellà  
311 2017. Zinc-finger proteins in health and disease. *Cell Death Discovery*. 3(1): 17071.
- 312 8. Chen SC., Jeng KS, and Lai MMC. 2017. Zinc Finger-Containing Cellular  
313 Transcription Corepressor ZBTB25 Promotes Influenza Virus RNA Transcription and  
314 Is a Target for Zinc Ejector Drugs. *Journal of Virology*. 91(20).
- 315 9. Chen XF, Wu J, Zhang YD, Zhang CX, Chen XT, Sun JH, Chen TX. 2018. Role of  
316 Zc3h12a in enhanced IL-6 production by newborn mononuclear cells in response to  
317 lipopolysaccharide. *Pediatrics & Neonatology*. 59(3):288-295. doi:  
318 10.1016/j.pedneo.2017.09.006. Epub 2017 Sep 21. PMID: 29054363.
- 319 10. .
- 320 11. Fehr AR and Perlman S. 2015. Coronaviruses: an overview of their replication and  
321 pathogenesis. *Methods in Molecular Biology*, 1282: 1-23.
- 322 12. Fu M and Blackshear PJ. 2017. RNA-binding proteins in immune regulation: a focus  
323 on CCCH zinc finger proteins. *Nature Reviews Immunology*, 17(2): 130-143.
- 324 13. Gao G., Guo X, and Goff SP. 2002. Inhibition of retroviral RNA production by ZAP,  
325 a CCCH-type zinc finger protein. *Science*, 297(5587): p. 1703-6.
- 326 14. Guo X, Carroll JW, Macdonald MR, Goff SP and Gao G. 2004. The zinc finger  
327 antiviral protein directly binds to specific viral mRNAs through the CCCH zinc finger  
328 motifs. *Journal of Virology*. 78(23): 12781-12787.
- 329 15. Hajikhezri Z, Darweesh M, Akusjärvi G, Punga T. 2020. Role of CCCH-Type Zinc  
330 Finger Proteins in Human Adenovirus Infections. *Viruses*. 18;12(11):1322. doi:  
331 10.3390/v12111322. PMID: 33217981; PMCID: PMC7698620.
- 332 16. Haneklaus M, O'Neil JD, Clark AR, Masters SL, O'Neill LAJ. 2017. The RNA-binding  
333 protein Tristetraprolin (TTP) is a critical negative regulator of the NLRP3  
334 inflammasome. *Journal of Biological Chemistry*. 28;292(17):6869-6881. doi:  
335 10.1074/jbc.M116.772947. Epub 2017 Mar 16. PMID: 28302726; PMCID:  
336 PMC5409458.
- 337 17. Kontoyiannis DL. 2018. An RNA checkpoint that keeps immunological memory at  
338 bay. *Nature Immunology*. 19(8): 795-797.
- 339 18. Kozaki T, Takahama M, Misawa T, Matsuura Y, Akira S, Saitoh T. 2015. Role of  
340 zinc-finger anti-viral protein in host defense against Sindbis virus. *International  
341 Immunology*. 27(7):357-64. doi: 10.1093/intimm/dxv010. Epub 2015 Mar 10. PMID:  
342 25758257; PMCID: PMC4565983.
- 343 19. Krishna SS., Majumdar I., and Grishin NV. 2003. Structural classification of zinc  
344 fingers: survey and summary. *Nucleic Acids Research* 31(2): 532-50.
- 345 20. Lai WS, Carballo E, Thorn JM, Kennington EA, Blackshear PJ. 2000. Interactions of  
346 CCCH zinc finger proteins with mRNA. Binding of tristetraprolin-related zinc finger  
347 proteins to Au-rich elements and destabilization of mRNA. *Journal of Biological  
348 Chemistry* 9;275(23):17827-37. doi: 10.1074/jbc.M001696200. PMID: 10751406.
- 349 21. Lai WS, Kennington EA and Blackshear PJ. 2003. Tristetraprolin and its family  
350 members can promote the cell-free deadenylation of AU-rich element-containing

- 351 mRNAs by poly(A) ribonuclease. *Molecular and Cellular Biology*, 23(11): p. 3798-  
352 812.
- 353 22. Lai WS, Stumpo DJ, Wells ML, Gruzdev A, Hicks SN, Nicholson CO, Yang Z, Faccio  
354 R, Webster MW, Passmore LA, Blackshear PJ. 2019. Importance of the Conserved  
355 Carboxyl-Terminal CNOT1 Binding Domain to Tristetraprolin Activity *In Vivo*.  
356 *Molecular and Cellular Biology*. 39(13):e00029-19. doi: 10.1128/MCB.00029-19.  
357 PMID: 31036567; PMCID: PMC6580703.
- 358 23. Lal S, Ullah BA, and Syed S. 2020. The Role of Zinc-Finger Antiviral Proteins in  
359 Immunity against Viruses. *Molecular Genetics, Microbiology and Virology*, 35(2):  
360 78-84.
- 361 24. Li M, Yan K, Wei L, Yang J, Lu C, Xiong F, Zheng C, Xu W. 2015. Zinc finger  
362 antiviral protein inhibits coxsackievirus B3 virus replication and protects against viral  
363 myocarditis. *Antiviral Research*. 123:50-61. doi: 10.1016/j.antiviral.2015.09.001.  
364 Epub 2015 Sep 2. PMID: 26343012.
- 365 25. Lin RJ, Huang CH, Liu PC, Lin IC, Huang YL, Chen AY, Chiu HP, Shih SR, Lin LH,  
366 Lien SP, Yen LC, Liao CL. 2020. Zinc finger protein ZFP36L1 inhibits influenza A  
367 virus through translational repression by targeting HA, M and NS RNA transcripts.  
368 *Nucleic Acids Research*. 27;48(13):7371-7384. doi: 10.1093/nar/gkaa458. PMID:  
369 32556261; PMCID: PMC7367194.
- 370 26. Lv L, Qin T, Huang Q, Jiang H, Chen F, Long F, Ren L, Liu J, Xie Y, Zeng M. 2021.  
371 Targeting Tristetraprolin Expression or Functional Activity Regulates Inflammatory  
372 Response Induced by MSU Crystals. *Frontiers in Immunology*. 16;12:675534. doi:  
373 10.3389/fimmu.2021.675534. PMID: 34335573; PMCID: PMC8322984.
- 374 27. Lykke-Andersen J. and Wagner E. Recruitment and activation of mRNA decay  
375 enzymes by two ARE-mediated decay activation domains in the proteins TTP and  
376 BRF-1. *Genes & Development*, 19(3): p. 351-61.
- 377 28. Maeda K. and Akira S. 2017. Regulation of mRNA stability by CCCH-type zinc-finger  
378 proteins in immune cells. *International Immunology*, 29(4): 149-155.
- 379 29. Matsushita K, Takeuchi O, Standley DM, Kumagai Y, Kawagoe T, Miyake T, Satoh  
380 T, Kato H, Tsujimura T, Nakamura H, Akira S. 2009. Zc3h12a is an RNase essential  
381 for controlling immune responses by regulating mRNA decay. *Nature*.  
382 30;458(7242):1185-90. doi: 10.1038/nature07924. Epub 2009 Mar 25. PMID:  
383 19322177.
- 384 30. Meagher J., Takata M, Gonçalves-Carneiro D, Keane SC, Rebendenne A, Ong H, Orr  
385 VK, MacDonald MR, Stuckey JA, Bieniasz PD and Smith JL. 2019. Structure of  
386 the zinc-finger antiviral protein in complex with RNA reveals a mechanism for  
387 selective targeting of CG-rich viral sequences. *Proceedings of the National Academy  
388 of Sciences*. 116(48): 24303-24309.
- 389 31. Mino T, Murakawa Y, Fukao A, Vandenbon A, Wessels HH, Ori D, Uehata T, Tartey  
390 S, Akira S, Suzuki Y, Vinuesa CG, Ohler U, Standley DM, Landthaler M, Fujiwara  
391 T, Takeuchi O. 2015. Regnase-1 and Roquin Regulate a Common Element in  
392 Inflammatory mRNAs by Spatiotemporally Distinct Mechanisms. *Cell*.  
393 21;161(5):1058-1073. doi: 10.1016/j.cell.2015.04.029. PMID: 26000482.
- 394 32. Müller S, Möller P, Bick MJ, Wurr S, Becker S, Günther S and Kümmerer BM. 2007.  
395 Inhibition of filovirus replication by the zinc finger antiviral protein. *Journal of  
396 virology*. 81(5): 2391-2400.

- 397 33. Musah RA 2004, The HIV-1 nucleocapsid zinc finger protein as a target of  
398 antiretroviral therapy. *Current Topics in Medicinal Chemistry*, 4 (15): 1605-22.
- 399 34. Reed LJ and Muench J. 1938. A simple method of estimating fifty percent endpoints..  
400 *American Journal of Epidemiology*.27(3): 493-497.
- 401 35. Schito ML, Soloff AC, Slovitz D, Trichel A, Inman JK, Appella E, Turpin JA and  
402 Barratt-Boyes SM. 2006. Preclinical evaluation of a zinc finger inhibitor targeting  
403 lentivirus nucleocapsid protein in SIV-infected monkeys. *Current HIV Research*. 4(3):  
404 379-386.
- 405 36. Schneider C., Rasband W. and Eliceiri K. 2012. NIH Image to ImageJ: 25 years of  
406 image analysis. *Nature Methods* 9, 671–675 (2012).  
407 <https://doi.org/10.1038/nmeth.2089>.
- 408 37. Scozzafava A., Owa T, Mastrolorenzo A and Supuran CT . 2003. Anticancer and  
409 antiviral sulfonamides. *Current Medicinal Chemistry*. 10(11): 925-953.
- 410 38. Shrestha A, Pun NT and Park PH. 2018.ZFP36L1 and AUF1 Induction Contribute to  
411 the Suppression of Inflammatory Mediators Expression by Globular Adiponectin via  
412 Autophagy Induction in Macrophages. *Biomolecules & Therapeutics*.26(5): 446-457.
- 413 39. Strober W. 2015. Trypan Blue Exclusion Test of Cell Viability. *Current Protocols in*  
414 *Immunology*. 2;111:A3.B.1-A3.B.3. doi: 10.1002/0471142735.ima03bs111. PMID:  
415 26529666; PMCID: PMC6716531
- 416 40. Stumpo DJ., Lai WS, and Blackshear PJ. 2010. Inflammation: cytokines and RNA-  
417 based regulation. *Wiley Interdisciplinary Reviews:RNA*, 1(1): 60-80.
- 418 41. Suk FM, Chang CC, Lin RJ, Lin SY, Liu SC, Jau CF, Liang YC. 2018. ZFP36L1 and  
419 ZFP36L2 inhibit cell proliferation in a cyclin D-dependent and p53-independent  
420 manner. *Scientific Reports*. 9;8(1):2742. doi: 10.1038/s41598-018-21160-z. Erratum  
421 in: *Sci Rep*. 2019 Nov 20;9(1):17457. PMID: 29426877; PMCID: PMC5807420.
- 422 42. Takata MA, Gonçalves-Carneiro D, Zang TM, Soll SJ, York A, Blanco-Melo D and  
423 Bieniasz PD. 2017. CG dinucleotide suppression enables antiviral defence targeting  
424 non-self RNA. *Nature*, 550(7674): 124-127.Tu Y, Wu X, Yu F, Dang J, Wang J, Wei  
425 Y, Cai Z, Zhou Z, Liao W, Li L, Zhang Y. 2019. Tristetraprolin specifically regulates  
426 the expression and alternative splicing of immune response genes in HeLa cells. *BMC*  
427 *Immunology*. 2;20(1):13. doi: 10.1186/s12865-019-0292-1. PMID: 31046669;  
428 PMCID: PMC6498542.
- 429 43. Tang Q, Wang X, and Gao G. 2017. The Short Form of the Zinc Finger Antiviral  
430 Protein Inhibits Influenza A Virus Protein Expression and Is Antagonized by the  
431 Virus-Encoded NS1. *Journal of Virology*, 91(2): p. e01909-16.
- 432 44. Uehata T. and Akira S. 2013. mRNA degradation by the endoribonuclease *Regnase-*  
433 *I/ZC3H12a/MCPIP-1*. *Biochimica et Biophysica Acta*, 1829 (6-7): p. 708-13.
- 434 45. Vilas CK, Emery LE, Denchi EL, Miller KM. 2018. Caught with One's Zinc Fingers  
435 in the Genome Integrity Cookie Jar. *Trend in Genetics*. 34(4):313-325. doi:  
436 10.1016/j.tig.2017.12.011. Epub 2018 Jan 19. PMID: 29370947; PMCID:  
437 PMC5878116.
- 438 46. Villa N, Do A, Hershey JW, Fraser CS. 2013. Human eukaryotic initiation factor 4G  
439 (eIF4G) protein binds to eIF3c, -d, and -e to promote mRNA recruitment to the  
440 ribosome. *Journal of Biological Chemistry*. 15;288(46):32932-40. doi:  
441 10.1074/jbc.M113.517011. Epub 2013 Oct 3. PMID: 24092755; PMCID:  
442 PMC3829144.

- 443 47. Wang KT, Wang HH, Wu YY, Su YL, Chiang PY, Lin NY, Wang SC, Chang GD,  
444 Chang CJ. 2015. Functional regulation of Zfp3611 and Zfp3612 in response to  
445 lipopolysaccharide in mouse RAW264.7 macrophages. *Journal of*  
446 *Inflammation*.16;12:42. doi: 10.1186/s12950-015-0088-x. PMID: 26180518; PMCID:  
447 PMC4502546.
- 448 48. Wawro M, Kochan J, and Kasza A, The perplexities of the ZC3H12A self-mRNA  
449 regulation. *Acta Biochimica Polonica*, 63(3): p. 411-5.
- 450 49. Wu HY, Ke TY, Liao WY, Chang NY. 2013. Regulation of coronavirus poly(A) tail  
451 length during infection. *PLoS One*. 29;8(7):e70548. doi:  
452 10.1371/journal.pone.0070548. PMID: 23923003; PMCID: PMC3726627.
- 453 50. Zhang B, Goraya MU, Chen N, Xu L, Hong Y, Zhu M and Chen JL .2020. Zinc Finger  
454 CCCH-Type Antiviral Protein 1 Restricts the Viral Replication by Positively  
455 Regulating Type I Interferon Response. *Frontiers in microbiology*. 11: 1912-1912.
- 456 51. Zhao Y, Song Z, Bai J, Liu X, Nauwynck H and Jiang P. 2019. ZAP, a CCCH-Type  
457 Zinc Finger Protein, Inhibits Porcine Reproductive and Respiratory Syndrome Virus  
458 Replication and Interacts with Viral Nsp9. *Journal of Virology*. 93(10).
- 459 52. Zhu M, Ma X, Cui X, Zhou J, Li C, Huang L, Shang Y, Cheng Z. 2017. Inhibition of  
460 avian tumor virus replication by CCCH-type zinc finger antiviral protein. *Oncotarget*.  
461 19;8(35):58865-58871. doi: 10.18632/oncotarget.19378. PMID: 28938603; PMCID:  
462 PMC5601699.
- 463 53. Zhu M., Zhou J, Liang Y, Nair V, Yao Y and Cheng Z. 2020. CCCH-type zinc finger  
464 antiviral protein mediates antiviral immune response by activating T cells. *Journal of*  
465 *Leukocyte Biology*. 107(2): 299-307.
- 466 54. Zhu Y, Chen G, Lv F, Wang X, Ji X, Xu Y, Sun J, Wu L, Zheng YT, Gao G. 2011.  
467 Zinc-finger antiviral protein inhibits HIV-1 infection by selectively targeting multiply  
468 spliced viral mRNAs for degradation. *Proceedings of the National Academy of*  
469 *Sciences of the United States of America*. 20;108(38):15834-9. doi:  
470 10.1073/pnas.1101676108. Epub 2011 Aug 29. PMID: 21876179; PMCID:  
471 PMC3179061.
- 472 55. Zhu Y, Wang X, Goff SP, Gao G. 2012. Translational repression precedes and is  
473 required for ZAP-mediated mRNA decay. *The EMBO Journal*. 5;31(21):4236-46. doi:  
474 10.1038/emboj.2012.271. Epub 2012 Sep 28. PMID: 23023399; PMCID:  
475 PMC3492732.
- 476  
477  
478  
479

# Figure 1

Overexpression and knockdown of ZFP36L1 in HCT-8 cells

Wild type HCT8 wells (A), ZFP36L1 overexpressed HCT-8 cells with GFP marker (B), and ZFP36L1 knockdown HCT-8 cells with mCherry marker (C). Overexpression and knockdown of ZFP36L1 were performed by lentivirus transduction.

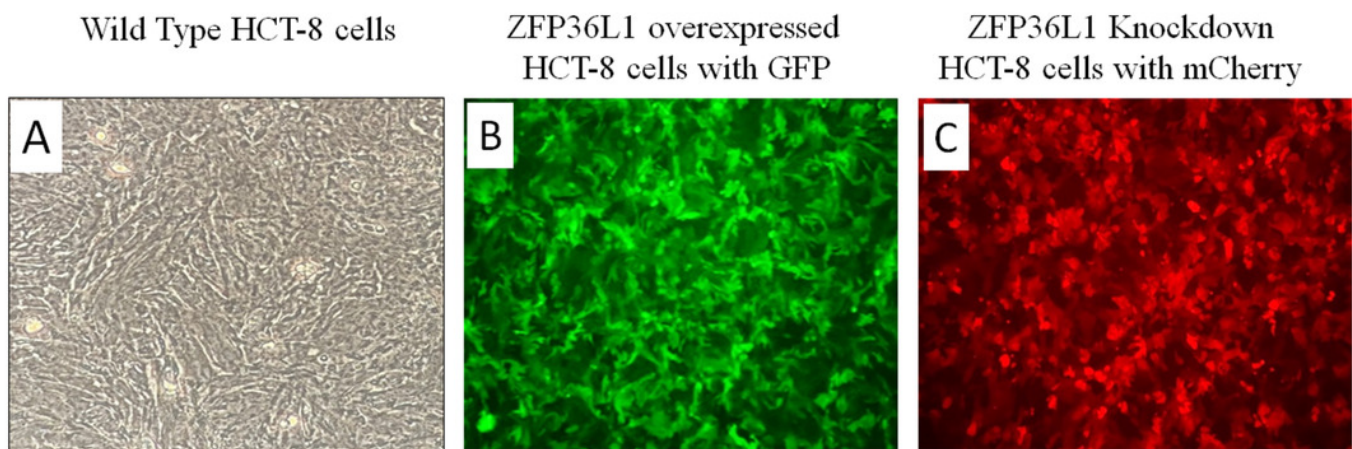


## Figure 2

Western blot for confirming ZFP36L1 overexpression and knockdown in HCT-8 cells

Cell lysate for wild type HCT-8 cell (A), ZFP36L1 overexpressed (B) and ZFP36L1 knockdown (C) were separated with 12% resolving SDS PAGE gel and transferred to PVDF membrane. Proteins on the membrane were detected with an anti-ZFP36L1 antibody and anti-  $\beta$ actin antibody with HRP-conjugated secondary antibodies.

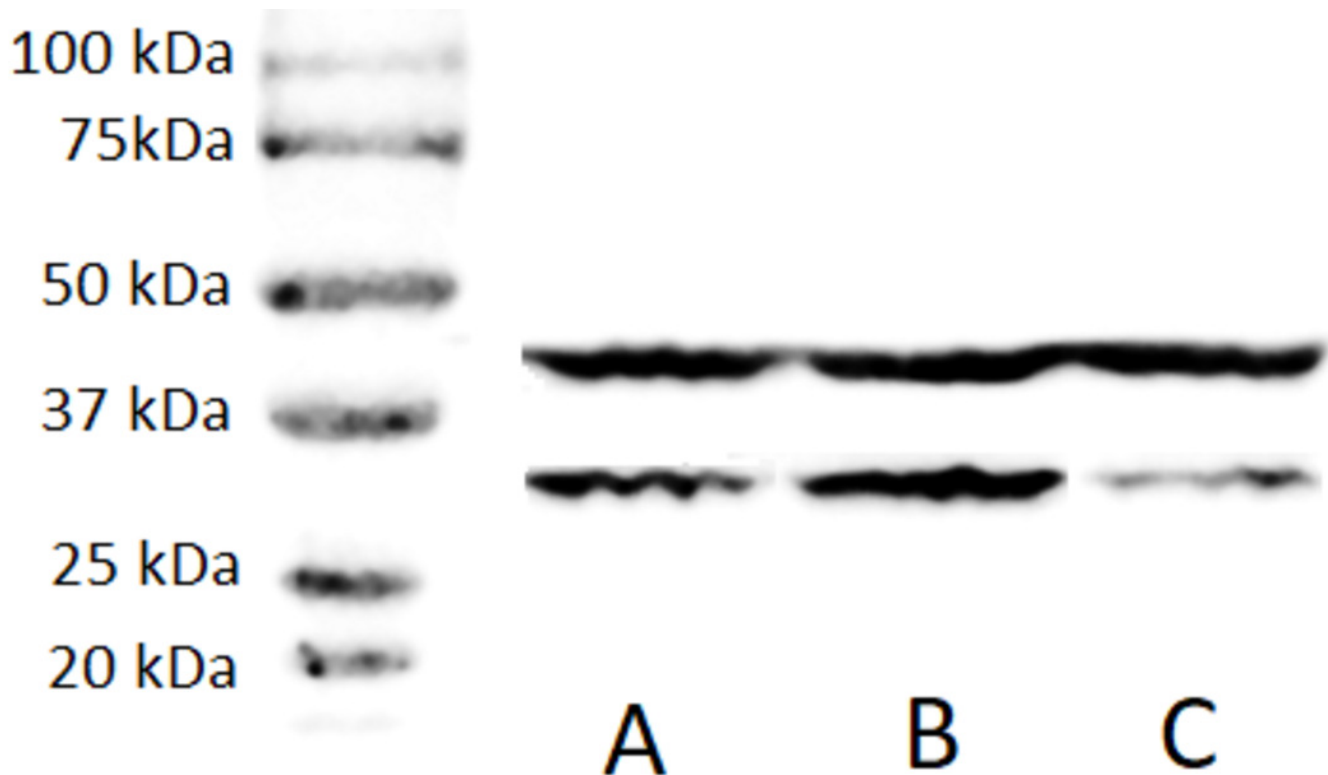


## Figure 3

Relative quantification of ZFP36L1 expression in HCT-8 cell following its overexpression and knockdown

Cell lysate for wild-type HCT-8 cell, ZFP36L1 overexpressed and ZFP36L1 knockdown was analyzed for ZFP36L1 and  $\beta$  actin using western blot. Band intensity for ZFP36L1 proteins was normalized with  $\beta$  actin using ImageJ software. A significant difference in ZFP36L1 expression in ZFP36L1 overexpressed and knockdown cells compared to wild-type cells was estimated using a paired T-test. Asterisks are showing significant differences in ZFP36L1 expression.

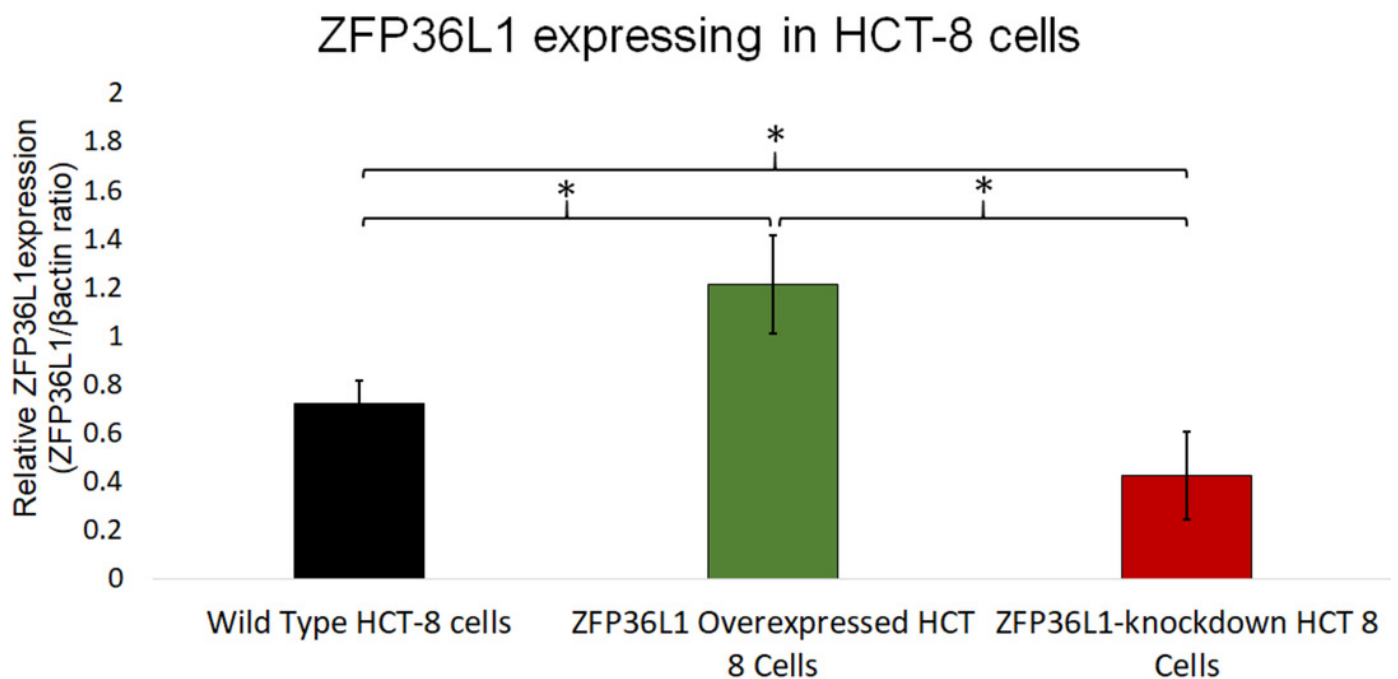


## Figure 4

### Effect of ZFP36L1 on HCT-8 cells viability

The effect of ZFP36L1 overexpression and its knockdown on cell viability was measured by trypan blue exclusion assay. Wild type, ZFP36L1 overexpressed and ZFP36L1 knockdown cells were individually seeded in 6 well plates. After 96 hours post-seeding, cells were detached and stained with 0.4% trypan blue to determine the percent viability. Changes in cell viability following ZFP36L1 overexpression or its knockdown compared to wild-type cells was estimated by paired T-test.

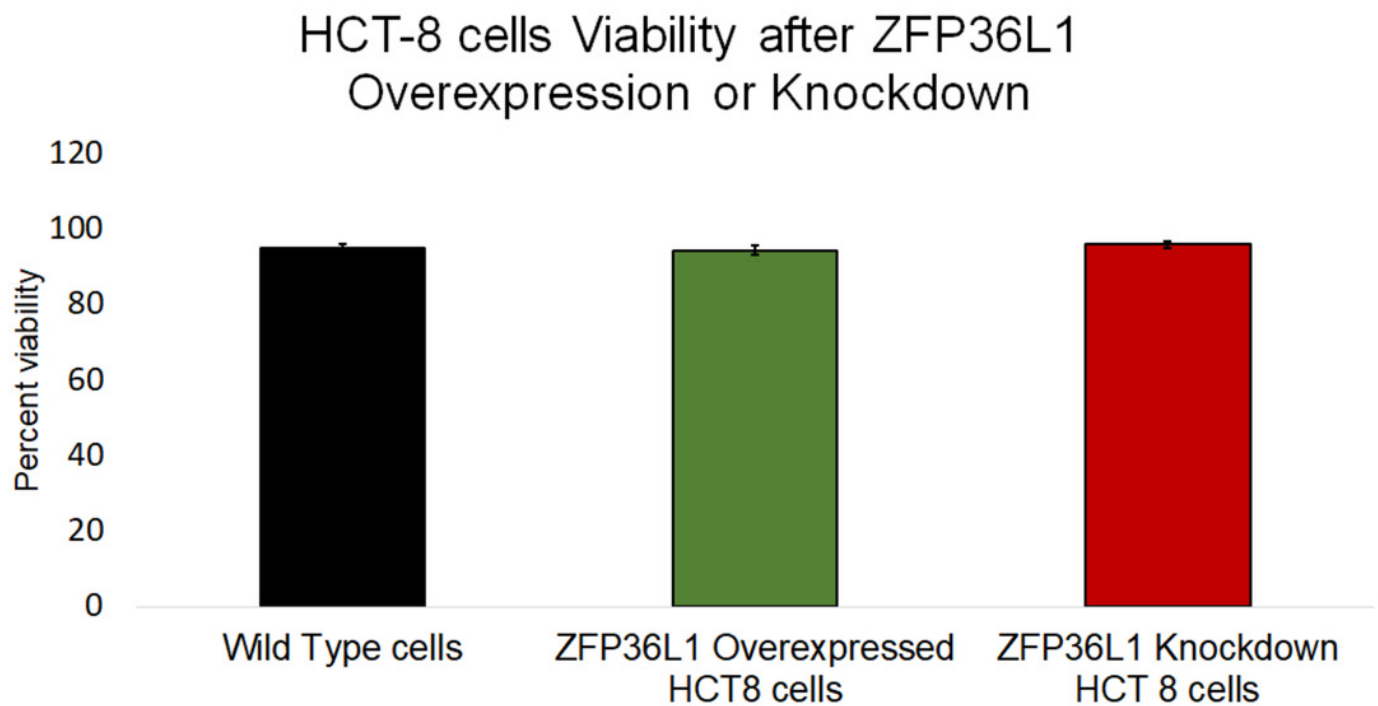


## Figure 5

Human coronavirus-OC43 titer in HCT-8 cells.

Wild type, ZFP36L1 overexpressed and ZFP36L1 knockdown HCT-8 cells were infected individually with HCoV-OC43 with 0.1 MOI. Supernatant from these cells was collected at 24 hours, 48 hours, 72 hours, and 96 hours p.i. and analyzed for virus titer. Asterisks are showing significant differences in virus titer.

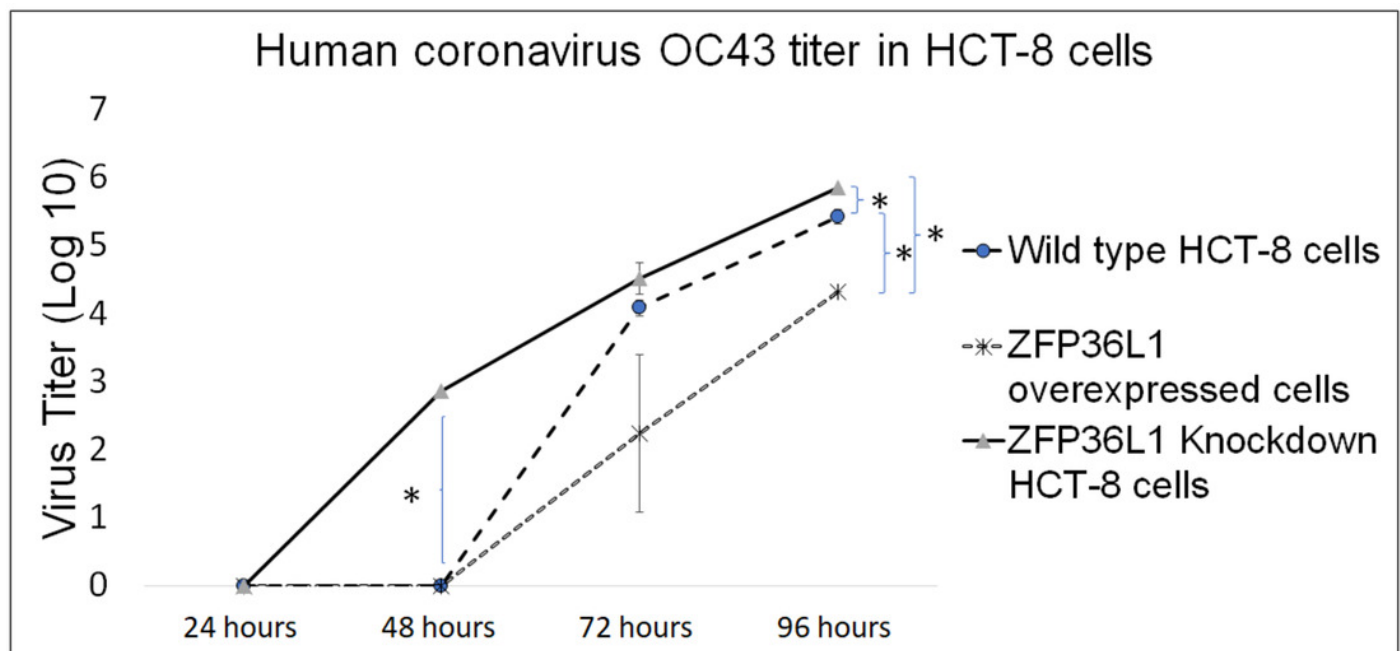


## Figure 6

Effect of ZFP36L1 expression on Human coronavirus-OC43 induced cytopathic effect in HCT-8 cells

Wild type, ZFP36L1 overexpressed and ZFP36L1 knockdown HCT-8 cells were infected individually with HCoV-OC43 with 0.1 MOI. Cytopathic effect was observed at 72 hours p.i. at 40X magnification

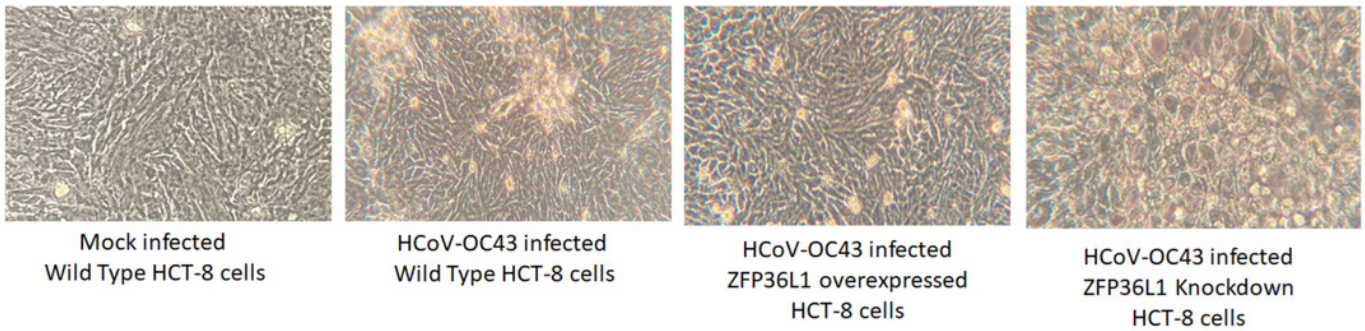


## Figure 7

### Effect of ZFP36L1 expression on Human coronavirus-OC43 replication

Wild-type, ZFP36L1 overexpressed and ZFP36L1 knockdown HCT-8 cells were infected individually with HCoV-OC43 with 0.1 MOI. Viral RNA was isolated from infected cells at 72 and 96 hours p.i. Isolated RNA was quantified using qPCR (for viral nucleocapsid). Fold change in nucleocapsid RNA in ZFP36L1 overexpressed and knockdown cells as compared to wild-type HCT-8 cells were estimated using paired T-test. Asterisks are showing significant differences in viral RNA.

